Carbohydrate Polymers 103 (2014) 434–441

Contents lists available at ScienceDirect

Carbohydrate Polymers

journal homepage: www.elsevier.com/locate/carbpol

Structural elucidation and *in vitro* antitumor activity of a novel oligosaccharide from *Bombyx batryticatus*

Xue Jiang[a], Zuofa Zhang[b], Yajie Chen[a], Zhenteng Cui[a], Liangen Shi[a,*]

[a] College of Animal Sciences, Zhejiang University, Hangzhou, Zhejiang 310058, China
[b] Institute of Horticulture, Zhejiang Academy of Agricultural Science, Hangzhou, Zhejiang 310021, China

ARTICLE INFO

Article history:
Received 22 August 2013
Received in revised form
13 December 2013
Accepted 14 December 2013
Available online 8 January 2014

Keywords:
Bombyx batryticatus
Oligosaccharide
Structural elucidation
Antitumor activity

ABSTRACT

An oligosaccharide BBPW-2 was isolated and purified from *Bombyx batryticatus*, its molecular weight was 2.0×10^3 Da, and its structure was elucidated by compositional, methylation and NMR analysis. Our results showed that BBPW-2 consisted of β-D-(1 → 2,6)-glucopyranose and β-D-(1 → 2,6)-mannosyl units serving as the backbone, α-D-(1 → 2)-galactopyranose and α-D-(1 → 3)-mannosyl units as branches, and α-D-Man*p* and β-D-Glc*p* as terminals. The *in vitro* inhibitory activity of BBPW-2 was measured using MTT and and crystal violet assays, which suggested that BBPW-2 had direct cytotoxic effects on the cancer cell lines HeLa and HepG2 (particularly HeLa cells), and had a long-term antiproliferative effect on MCF-7 cells, respectively. Apoptosis and cellcycle analysis of HeLa cells showed that BBPW-2 induced cellcycle disruption in the G0/G1 and G2/M phases accompanied by an impressive increment of early apoptotic cells and late apoptotic and necrotic cells. These results suggest that BBPW-2 could be a potential chemotherapeutic drug and its antitumor effects deserve further study.

1. Introduction

Bombyx batryticatus is an oriental crude drug, composed of dried silkworm larvae, *Bombyx mori* L., dead and stiffened by infection with *Beauveria bassiana* (Kikuchi, Takahashi, & Oshima, 2004; Kim et al., 2001). In traditional Chinese medical applications, *B. batryticatus* is used for treating headaches, convulsions, tonsillitis, Bell's palsy, asthma, and thyroid adenoma (Kwon et al., 2003). Polysaccharides are widely distributed in animals, plants, and microorganisms. Pharmacological studies have shown that polysaccharides possess a number of biological activities including immunoregulation (Kodama, Murata, & Nanba, 2004), anti-inflammation (Liao, Guo, & Lin, 2011), antioxidation (Cui, Yuan, & Zhang, 2010), and antitumor (Chen et al., 2004) among others. In recent years, structural and pharmacological research on plant and fungus polysaccharides is a hot topic (Kim et al., 2006; Kodama et al., 2004; Zhang, Xu, Fu, & Sun, 2013). However, there are no reports on polysaccharides from *B. batryticatus*.

As a major active constituent, polysaccharide plays an important role in the pharmacologic actions of *B. batryticatus*. *B. batryticatus* is a complex of fungi and silkworm larvae, whose polysaccharide may be more sophisticated and efficacious than plant polysaccharide. Thus it is necessary to separate and purify the polysaccharide from *B. batryticatus* and investigate its pharmacological activities. To our knowledge, this is the first study on the purification, structural elucidation and *in vitro* antitumor of activities of polysaccharide from *B. batryticatus*.

2. Materials and methods

2.1. Materials and reagents

Silkworm larvae of strain Qiufeng × Baiyu were reared in mass on mulberry leaves up to the fourth molt. An inoculum of *B. bassiana* containing approximately 1×10^7 conidia/mL was surface-applied onto newly fourth-exuviated larvae that were reared continuously under more favorable circumstances (25 °C, humidity 90%). Dead mummified larvae were collected and kept till they were covered with white conidiophores. When used, *B. batryticatus* were freeze-dried and comminuted.

DEAE-Sepharose Fast Flow and High-Resolution Sephacryl S-200 and S-300 were purchased from GE Healthcare. Standard monosaccharides (L-fucose, L-rhamnose, D-manonose, D-xylose, D-glucose, D-galactose and D-arabinose), dextrans, trifluoroacetic acids (TFA), and dimethyl sulfoxide (DMSO) were bought from Sigma–Aldrich. Three cancer cell lines were obtained from Cell

* Corresponding author. Tel.: +86 571 88982723; fax: +86 571 88982723.
E-mail address: slgsilk@zju.edu.cn (L. Shi).

0144-8617/$ – see front matter © 2014 Published by Elsevier Ltd.
http://dx.doi.org/10.1016/j.carbpol.2013.12.039

Bank of Institute of Biochemistry and Cell Biology, Chinese Academy of Science (Shanghai, China): HeLa (human cervical carcinoma), HepG2 (human hepatoma), and MCF-7 (human breast adenocarcinoma). DMEM medium and fetal bovine serum (FBS) was obtained from Thermo Scientific (Hyclone). Annexin V-FITC apoptosis detection kit was bought from Multisciences. 3-(4,5-dimethyl-thiazol-2-yl)-2,5-diphenyl tetrazolium bromide (MTT), 5-fluorouracil (5-Fu), crystal violet, RNase A, and propidium iodide (PI) were obtained from Sangon Biotech. All other reagents were at the highest commercial grade from Huadong Chemical Reagent Co. Ltd. (Hangzhou, China).

2.2. Extraction, isolation and purification of BBPW-2

Dried *B. batryticatus* powder was defatted with petroleum ether for 1 h, and the residue was dried and extracted twice with 80% ethanol for 1 h to remove small molecule sugar, glycoside and alkaloid, etc. Residue was dried at 40 °C and extracted with distilled water for 1.5 h at 100 °C. The suspension was centrifuged (4000 × *g*, 15 min), insoluble material was treated again as mentioned above. The supernatant was incorporated and concentrated to one-fifth of the initial volume using a rotary evaporator at 50 °C under vacuum. The supernatant was precipitated with four volumes of 95% (v/v) ethanol for 48 h at 4 °C. The precipitates were isolated by centrifugation (3000 × *g*, 10 min), washed with acetone and dried under reduced pressure at −80 °C to obtain crude polysaccharides. These crude polysaccharides were subjected to the Sevag method (4:1 chloroform:butyl alcohol) to remove free proteins. The deproteinated solution was re-precipitated with four volumes of 95% ethanol. The precipitate was collected by centrifugation and lyophilization, and then polysaccharide of *B. batryticatus* was obtained and named BBPS.

BBPS solution was applied to a DEAE-Sepharose Fast Flow Column (XK 26 mm × 100 cm), and gradient eluted with distilled water, 0.1 M, 0.2 M, 0.4 M NaCl solutions. Each fraction was collected and determined by phenol–sulfuric acid assay (Dubois, Gilles, Hamilton, Rebers, & Smith, 1956). BBPW was obtained from distilled water elution and subsequently purified by columns of Sephacryl S-300 and S-200 High Resolution (XK 26 mm × 100 cm) subsequently. Two absorption peaks were detected with a refractive index detector, and the second peak was collected and named BBPW-2.

2.3. Physicochemical characterisation of BBPW-2

2.3.1. Determination of BBPW-2 purity and molecular weight

The homogeneity and molecular weight of purified BBPW-2 were determined by a Waters 1525 HPLC system equipped a 1525 pump and 2414 refractive index detector. An analytical column, TSK PWXL G4000, was applied. Distilled water was used as the mobile phase with a flow rate of 1.0 mL/min. The system was kept at 35 °C. Taking the elution time and the logarithm of molecular weight as the *X*- and *Y*-axis, respectively, the standard curve was constructed to estimate BBPW-2's molecular mass with T-series Dextran standards (Mw: 50 kDa, 80 kDa, 150 kDa, 270 kDa, 670 kDa, 1400 kDa, 2000 kDa).

2.3.2. Monosaccharide composition

BBPW-2 (2 mg) was treated with 2 M TFA at 120 °C for 6 h. The sugars in the hydrolysate were converted to their alditol acetates and analyzed by GC on an Agilent 6890N GC equipped with an Agilent column (30 m × 250 μm × 0.25 μm). The temperature program was as follows: the oven temperature started at 120 °C, increased at a rate of 10 °C/min and ended at 240 °C for 7 min. Helium carrier gas was at 1.5 mL/min, flame ionization detector (FID) was at 280 °C.

2.3.3. Linkage analysis

NaOH-DMSO suspension (25 mg/mL) was prepared (Anumula & Taylor, 1992) first. Dried BBPW-2 (2 mg) was dissolved in DMSO and methylated by 0.6 mL NaOH-DMSO and 0.6 mL iodomethane. Completely methylated BBPW-2 was extracted by $CHCl_3$ and evaporated to dryness, showing no absorption peak at the –OH band in the 3700–3200 cm^{-1} region. The sample was then hydrolyzed by 2 M TFA at 100 °C for 6 h, reducted by $NaBH_4$, and acetylated by Ac_2O. Finally the methylated alditol acetates were re-dissolved in $CHCl_3$ and analyzed by GC-MS.

2.3.4. UV and FT-IR analysis

UV–visible spectral analysis was performed on a UV spectrophotometer (UV-2550, Shimadzu) in the 200–400 nm region. The organic functional groups of the polysaccharides BBPW-2 were identified using an FTIR spectrophotometer (FTIR-8400S, Shimadzu) in the 4000–400 cm^{-1} region using the KBr pressed-disc method. The methylated BBPW-2 sample was analyzed directly in the same range to check if it was methylated completely.

2.3.5. Nuclear magnetic resonance (NMR) analysis

BBPW-2 was dissolved in D_2O in a NMR tube and lyophilized 3 times. All spectra including ^1H NMR (25 °C, 60 °C), ^{13}C NMR, DEPT, COSY, TOCSY, NOESY, HMQC and HMBC NMR spectra were determined by a Varian INOVA 500 Hz NMR spectrometer. ^1H chemical shifts were referenced to residual HDO at δ4.78 ppm (25 °C) as the internal standard and DSS (δ_C 0.00 ppm) as the external standard. COSY, TOCSY and HMQC spectra were used to assign the signals of chemical shifts. HMBC and NOESY spectra were used to assign the inter-residue linkage sequence.

2.4. Anticancer activity

2.4.1. Cell lines and culture

HeLa, HepG2, and MCF-7 cancer cell lines were maintained in DMEM medium supplemented with 10% (v/v) FBS in an incubator (Thermo Electron Corporation, MA, USA) with a humidified 5% CO_2 at 37 °C. Culture broths were substituted with fresh medium every 2 or 3 days. BBPW-2 solutions were prepared in DMEM medium.

2.4.2. MTT assay

The inhibitory effects of BBPW-2 on growth of HeLa and HepG2 cells were evaluated *in vitro* by MTT assay (Gan, Ma, Jiang, Xu, & Zeng, 2011). Briefly, cells were seeded in 96-well plates at 1×10^5 cells/well containing 100 μL culture medium each well and permitted to adhere for 24 h. 100 μL of BBPW-2 solutions with different concentrations (0.05 mg/mL, 0.10 mg/mL, 0.50 mg/mL, 1.0 mg/mL, 1.5 mg/mL, 2.0 mg/mL, and 2.5 mg/mL) and 5-Fu (25 μg/mL) were added to each well. After 72 h incubation, the BBPW-2/medium was removed and 100 μL of MTT (0.5 mg/mL, DMEM without FBS) was added. After further incubation at 37 °C for 4 h, the supernatant was aspirated and 150 μL of DMSO were added to each well. Absorbance was measured at 570 nm (A_{570}) by a 96-well microplate reader. All experiments were performed in quadruplicate. Growth inhibition rate was calculated as a percentage as follows: Growth inhibition rate (%) = $(1 - A_{experiment}/A_{control}) \times 100\%$.

2.4.3. Crystal violet assay

Crystal violet staining intensity is directly proportional to the number of adherent cells (Flick & Gifford, 1984), and was employed to observe the long-term antiproliferative effect of BBPW-2. According to the method by Mao et al. (2011), MCF-7 cells were seeded in six-well plates at 1×10^5 cells/well and cultured for 8 days with 5-Fu and different concentrations of BBPW-2/medium (0.05 mg/mL, 0.5 mg/mL, 1.0 mg/mL, and 2.0 mg/mL).

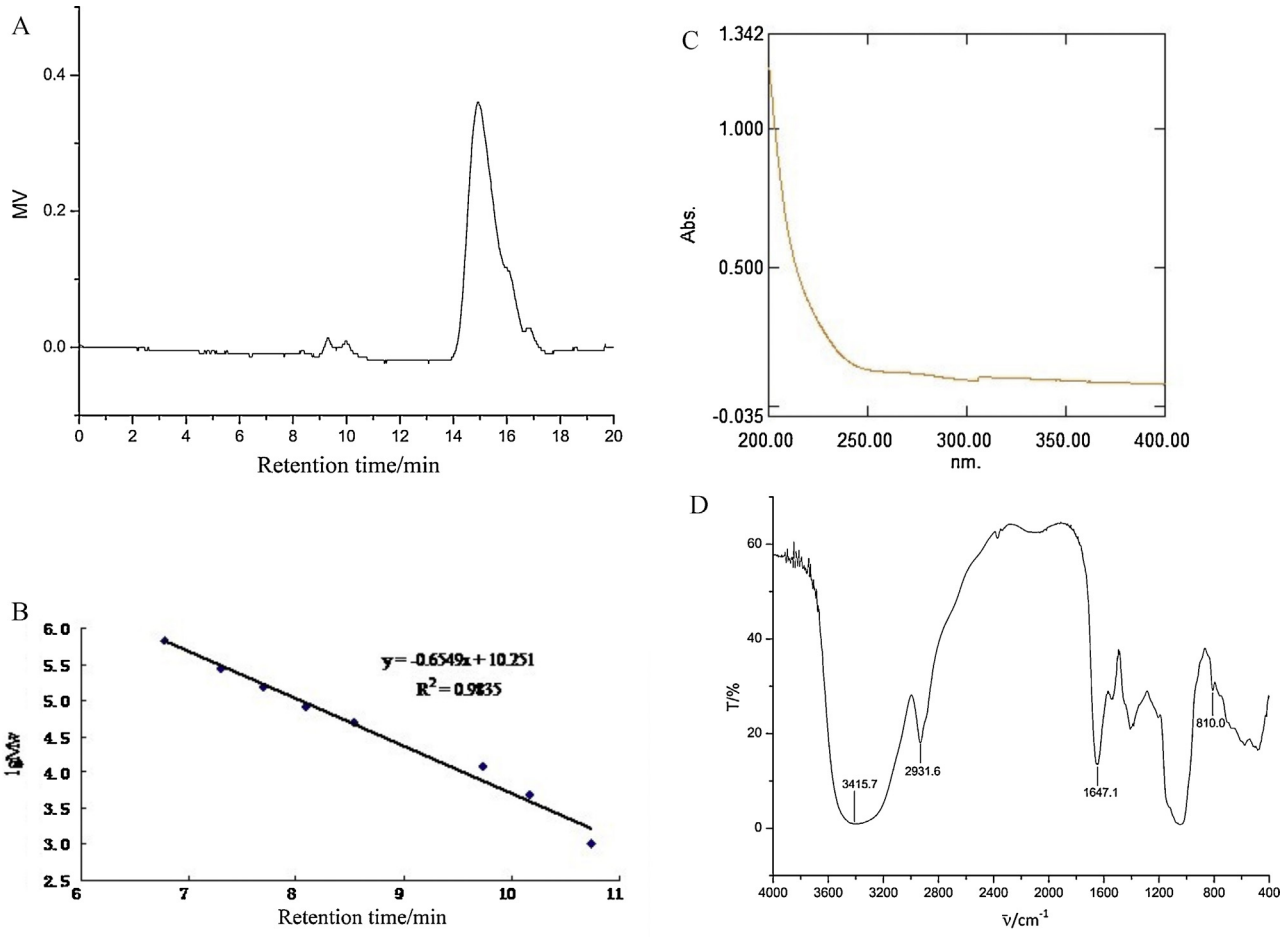

Fig. 1. HPLC elution of BBPW-2 (A) and standard curve of dextran series for measuring weight of BBPW-2 with HPLC (B), and the UV scanning curve (C) and FT-IR spectrum (D) of BBPW-2.

BBPW-2/medium was removed gently. A glutaraldehyde solution (1%, 2 mL) was prepared in PBS and added to each well to fix the cells for 15 min at room temperature. This solution was removed and replaced by 2 mL of a 0.02% aqueous solution of crystal violet. After 30 min incubation at room temperature, the staining solution was discarded, the plate was washed mildly with tap water and 2 mL of 70% ethanol was added to release the crystal violet. Finally, $A_{570\,nm}$ was measured by a microplate reader.

2.4.4. Apoptosis analysis

Apoptosis was monitored using the Annexin V-FITC/PI double fluorescence apoptosis detection kit (Wu et al., 2012) on a FACSCalibur flow cytometer. HeLa cells ($\approx 5 \times 10^6$) were treated with 7 mL BBPW-2/medium for 48 h in a 10 cm dish 24 h after adherence. Both of BBPW-2/medium and adherent cells were collected, total cells were harvested by centrifugation, then resuspended in 500 μL Annexin V-FITC binding buffer (1×). Annexin V-FITC (5 μL) and PI (10 μL) were added in sequence, this suspension was gently shaken and incubated for 5 min in the dark. Finally the percentage of cells in each group (living, early apoptosis, and late apoptosis and necrosis) was calculated by the FACS-Station System. Experiments were performed in triplicate.

2.4.5. Cellcycle analysis

The proportion of cells at different phases of cellcycle was also monitored by a FACSCalibur flow cytometer according the previously published method (Xie et al., 2013) with modifications. HeLa cells were treated and harvested as described in "Section 2.4.4". Cells were resuspended in 1 mL cold PBS, and then quickly injected to 3 mL pre-cooling ethanol at −20 °C with a sterilized syringe and placed at 4 °C overnight to fix the cells. Ethanol was removed by centrifugation, and cells were washed with PBS three times by centrifugation. RNase A (50 μg/mL, 500 μL) was added and incubated at 37 °C for 30 min, followed by addition of 500 μL of 50 μg/mL PI. Cells were incubated at 37 °C for another 30 min in the dark. Finally the distribution of cells at various cellcycle stages was determined by the flow cytometry.

2.4.6. Statistical analysis

All experiments were carried out in triplicate and data were expressed as mean ± standard deviation. Statistical analysis was performed by one-way analysis of variance (ANOVA). Statistical significance of the differences between groups was assessed by Student's *t*-test. All calculations were performed in the SAS 9.0. A level of $P < 0.05$ was considered statistically significant.

3. Results and discussion

3.1. Physicochemical properties of BBPW-2

The polysaccharide fraction BBPW-2 was purified by DEAE Sepharose anion-exchange chromatography and Sephacryl S-300 and S-200 high resolution chromatography. This product showed a single relatively symmetrical peak by HPLC (Fig. 1A), indicating its homogeneity. According to the standard curve (Fig. 1B) lgMw = −0.6549 Rt + 10.251 (Rt was the retention time), its

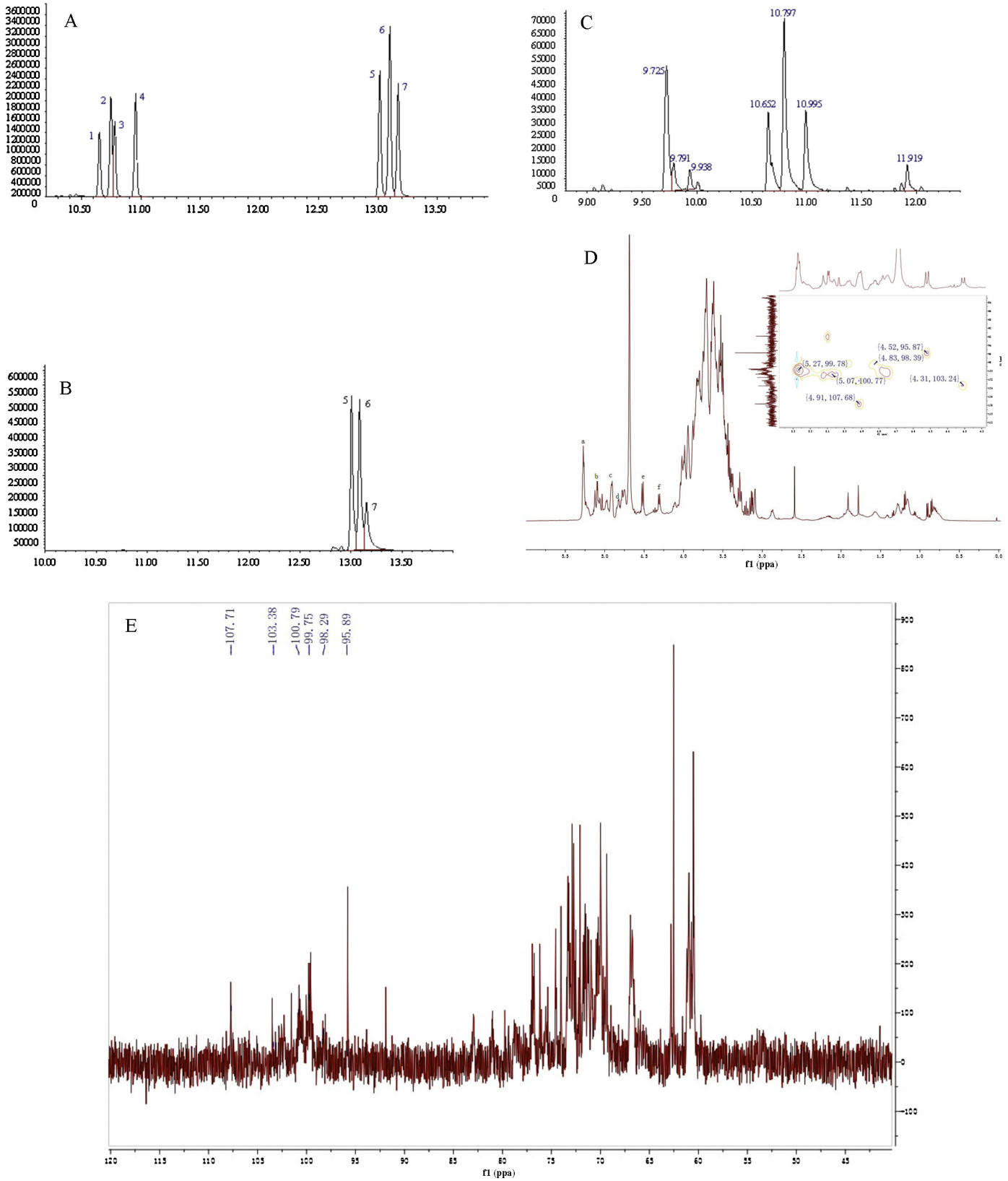

Fig. 2. Gas chromatogram profiles of the acetylated complex of standard monosaccharides (A) and BBPW-2 (B) and the methylated BBPW-2 derivant (C); and 500 MHz 1H (D) and 13C (E) NMR spectrum of BBPW-2.

molecular weight was ≈2.0×10^3 Da. No absorption was observed at 280 nm by UV scanning (Fig. 1C) and 1730 cm^{-1} in the FT-IR spectrum (Fig. 1D), showing that BBPW-2 is an oligosaccharide without protein and uronic acids. In the FT-IR spectrum, the large absorption peak at 3415.7 cm^{-1} and the weaker absorption at 2931.6 cm^{-1} could be the stretching vibrations of hydrogen-bonded OH groups and the C–H stretching vibrations of the free sugar, respectively. The absorption band at 1647 cm^{-1} was attributed to the hydration

Table 1
GC-MS data for methylation analysis of BBPW-2.

Rentent time	Methylated sugars	Substituted sugar unit	Molar ratios	Major mass (*m*/*z*)
9.725	2,3,4,6-Me_4-D-Man*p*	1-D-Man*p*	0.755	59, 71, 87, 101, 117, 129, 145, 161, 173, 205
9.789	2,4,6-Me_3-D-Gal*p*	1,3-D-Man*p*	0.178	53, 71, 101, 129, 161, 205, 277
9.936	2,3,4,6-Me_4-D-Glc*p*	1-D-Glc*p*	0.085	53, 71, 87, 101, 117, 129, 145, 161, 205
10.650	3,4,5,6-Me_4-D-Gal*p*	1,2-D-Gal*p*	0.533	59, 71, 87, 101, 113, 129, 145, 161, 189
10.794	3,4-Me_2-Glc*p*	1,2,6-D-Glc*p*	1.000	55, 71, 87, 101, 117, 131, 161, 189, 203, 233
10.994	3,4-Me_2-D-Man*p*	1,2,6-D-Man*p*	0.516	57, 71, 87, 101, 117, 131, 145, 161, 189, 233
11.920	3,4,6-Me_3-D-Gal*p*	1,2-D-Gal*p*	0.148	60, 71, 87, 99, 117, 129, 159, 189

vibration of BBPW-2. The weak absorption at 810 cm^{-1} indicated that BBPW-2 contained galactopyranose.

3.2. Monosaccharide composition and linkage analysis

Monosaccharide compositions of BBPW-2 were determined by acetylation and GC-MS analysis. GC chromatogram profiles of a standard monosaccharide mixture solution (Fig. 2A) and acetylated BBPW-2 (Fig. 2B) are shown in Fig. 2, revealing that BBPW-2 was composed of D-mannose, D-glucose, and D-galactose with a molar ratio of 1:0.74:0.59.

Methylation analysis (Fig. 2C, Table 1) indicated that the linkage types in BBPW-2 were composed of 1-D-Man*p*, 1,3-D-Man*p*, 1-D-Glc*p*, 1,2-D-Gal*p*, 1,2,6-D-Glc*p*, 1,2,6-D-Man*p*, at a ratio of 0.755:0.178:0.085:0.681:1.000:0.516:0.148, indicating that BBPW-2 is branched with terminal mannopyranose and glucopyranose residue, 2,6-disubstituted mannopyranose and glucopyranose residue, 2-substituted galactopyranose, and 3-substituted mannopyranose at the branching point. The total ratio of monosaccharide residues (D-mannose, D-glucose, and D-galactose) with different linkage types was 1:0.75:0.47, which was concordant with the results from monosaccharide analysis.

3.3. NMR analysis

The ^1H NMR (Fig. 2D) and ^{13}C NMR (Fig. 2E) spectra of BBPW-2 showed signals for six anomeric protons at δ4.31∼5.27 and six anomeric carbons at δ91.8∼107.9. Table 2 shows the chemical shifts data for BBPW-2 which were deduced as follows.

Residue **a** α-D-Man*p*. ^1H resonances for H-1, H-2, H-3 and H-4 were assigned from the cross-peaks in ^1H–^1H COSY, TOCSY and NOESY spectra. H-5, H-6a and H-6b were assigned from ^1H–^1H COSY spectrum. The corresponding ^{13}C resonances were assigned from the HMQC spectrum. In the NOESY spectrum, there was an H-1/H-2 intra-residue correlation. The shifts for $\delta_{H\text{-}5}$ and $\delta_{C\text{-}5}$ (3.83 and 73.2, respectively) were consistent with those of known standard α-mannopyranose (Jansson, Kenne, & Widmalm, 1989), indicating that residue **a** was identified as α-configuration. The downfield of the C-1 carbon signal with respect to the standard value for glycopyranoses indicated that residue **a** was α-D-Man*p*.

Residue **b** →2)-α-D-Gal*p*. ^1H resonances for H-1 to H-4 were assigned from the cross-peaks in the ^1H–^1H COSY and NOESY spectra. H-5, H-6a and H-6b were assigned from ^1H–^1H COSY, TOCSY and NOESY spectra. The cross-peaks of H-1/C-1 and H-1/C-5 in HMBC showed that H-5 and H-6 are located on residue **b**. The H-4/H-5 coupling constant was small in the NOESY spectrum, indicating a Gal-type residue (Staaf, Urbina, Weintraub, & Widmalm, 1999). The H-1/H-2 cross peak in NOESY spectrum, the small coupling constant ($J_{H\text{-}1,\,H\text{-}2}$ = 3.50 Hz), and the cross peaks of H-1/C-3 and H-1/C-5 in HMBC indicated that residue **b** is α-configuration. The downfield of the C-1 and C-2 carbon signals compared to the standard value for glycopyranoses indicated that residue **b** can be identified as →2)-α-D-Gal*p*.

Residue **c** →2,6)-β-D-Man*p*. The ^1H resonances for H-1 to H-4 were assigned from the cross-peaks in the ^1H–^1H COSY and TOCSY spectra. H-5, H-6a and H-6b were assigned from the ^1H–^1H COSY and NOESY spectra. In contrast to residue **a**, the shifts of $\delta_{H\text{-}5}$ and $\delta_{C\text{-}5}$, (3.54 and 76.8, respectively) were consistent with previously published data on standard β-mannopyranose (Jansson et al., 1989), indicating a β-configuration. The downfield of the C-1 and C-2 carbon signals indicated residue **c** was β-D-Man*p*.

Residue **d** →3)-α-D-Man*p*. With the same method to residue **a**, residue **d** was identified as →3)-α-D-Man*p*.

Residue **e** →2,6)-β-D-Glc*p*. Chemical shifts of residue **d** were assigned according to ^1H–^1H COSY and TOCSY spectra. All the cross-peaks were clearly visible, revealing that residue **e** was a gluco-configuration. H-1 appears a doublet ($J_{H\text{-}1,\,H\text{-}2}$ = 8.00 Hz), and its chemical shift is less than 4.8 ppm, indicating a β-configuration. The downfield of the C-1, C-2 and C-5 carbon signals indicated that residue **e** was →2,6)-β-D-Glc*p*.

Residue **f** β-D-Glc*p*. Similar to residue **e**, residue **f** appears as a β-gluco-configuration (H-1, doublet; $J_{H\text{-}1,\,H\text{-}2}$ = 8.00 Hz). The downfield of the C-1 carbon signal indicated residue **f** was β-D-Glc*p*.

The sequence of the glycosyl residue was derived from NOESY spectrum followed by confirmation with HMBC spectrum. Inter-residue NOE correlations (Table 3) were observed between H-1 of

Table 2
Chemical shifts data for BBPW-2.

Residue	Proton and carbon						
	1	2	3	4	5	6a	6b
α-D-Man*p*(**a**)	5.27	3.50	3.46	3.54	3.82	3.62	3.72
	99.8	71.6	71.7	66.7	73.2	60.4	
→2)-α-D-Gal*p*(**b**)	5.10	3.43	3.82	3.98	4.02	3.63	3.72
	100.7	**77.1**	73.2	74.5	69.9	60.9	
→2,6)-β-D-Man*p*(**c**)	4.92	3.94	3.72	3.86	3.54	3.69	3.75
	107.6	**82.7**	70.9	73.2	76.8	**66.2**	
→3)-α-D-Man*p*(**d**)	4.83	3.43	3.86	3.54	3.78	3.65	3.73
	98.4	71.5	**78.8**	66.8	69.6	61.6	
→2,6)-β-D-Glc*p*(**e**)	4.52	3.14	3.63	3.49	3.85	3.43	3.52
	95.9	**73.9**	76.1	71.9	78.8	**67.7**	
β-D-Glc*p*(**f**)	4.31	3.37	3.56	3.56	3.44	3.43	3.52
	103.2	76.3	72.6	72.6	71.6	62.7	

Bold numbers represent glycosylation sites.

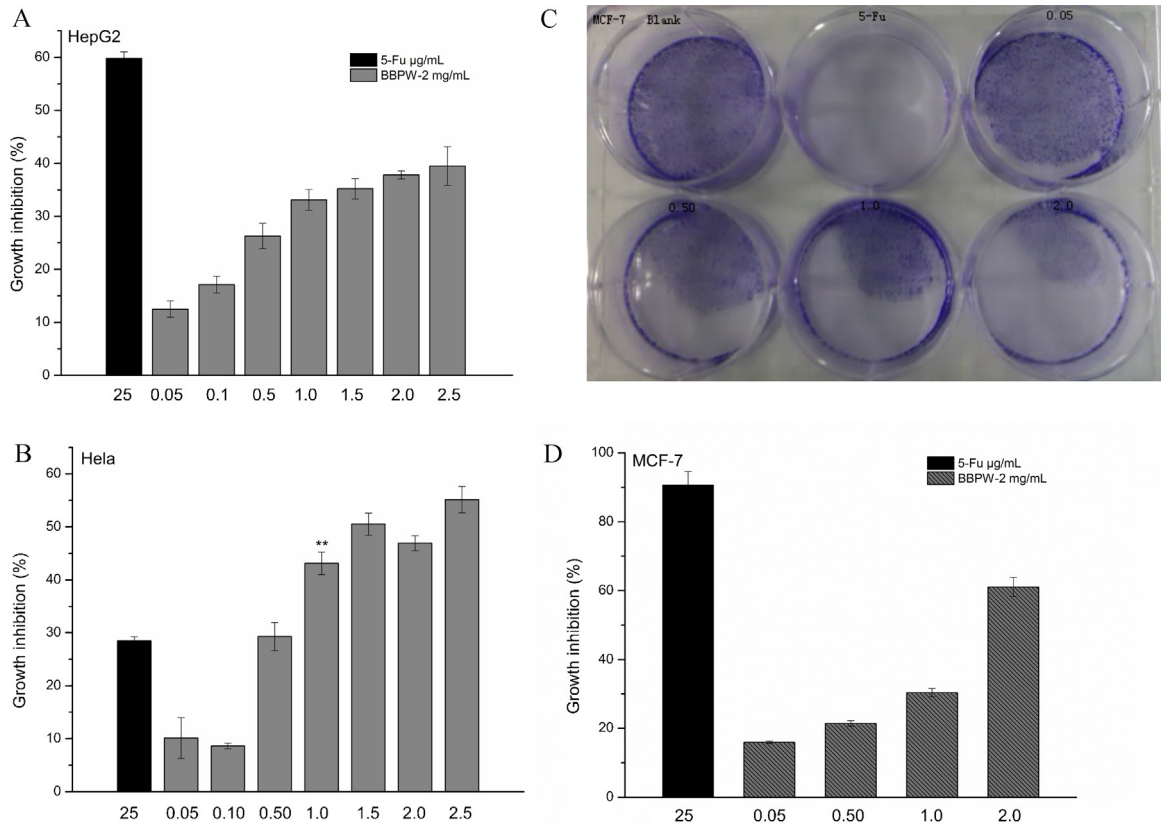

Fig. 3. Anticancer activities of BBPW-2: growth inhibitory effect of BBPW-2 on HepG2 (A) and HeLa cells (B) treated by BBPW-2 for 72 h; crystal violet assay measures the long-term growth inhibitory effect on MCF-7 cells treated by BBPW-2 for 8 days (C, D). (For interpretation of the references to colour in this figure legend, the reader is referred to the web version of the article.)

residue **a** and H-3 and H-4 of residue **d**, between H-1 of residue **c** and H-4 and H-5 of residue **b**, between H-1 of residue **d** and H-2 of residue **e**, between H-1 of residue **e** and H-3 of residue **a**, H-5 of residue **b**, between H-1 of residue **f** and H-4 of residue **b**. HMBC spectrum showed correlations between H-1 of residue **a** and C-5 of residue **c**, between H-1 of residue **c** and C-4 of residue **a**, C-3 of residue **d**, between H-1 of residue **d** and C-3 of residue **f**, between H-1 of residue **e** and C-4 of residue **a** and **b**, C-2 of residue **f**, between H-1 of residue **f** and C-4 of residue **b** (Table 4).

Combining all chemical and NMR data, the structure of BBPW-2 can be expressed as follows:

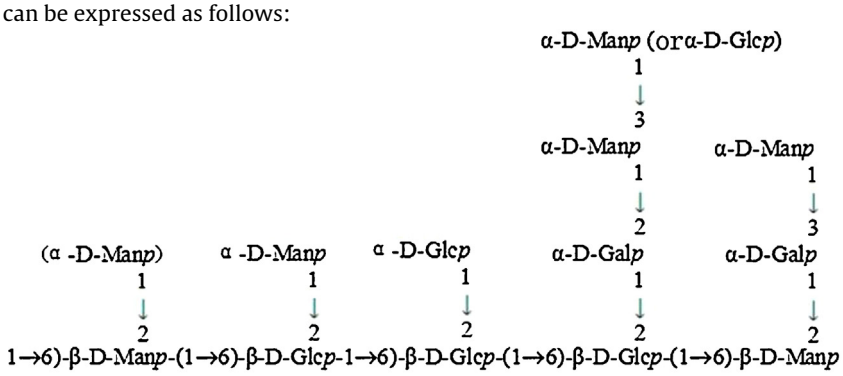

3.4. Anticancer activity

The *in vitro* antiproliferative activity of BBPW-2 on HepG2 and HeLa cells were investigated. As shown in Fig. 3, BBPW-2 exerted a concentration-dependent inhibitory effect on both cell lines treated for 72 h. The inhibition rates were 39.5% (Fig. 3A) and 55.1% (Fig. 3B) at the highest dose of 2.5 mg/mL for HepG2 and HeLa cells, respectively. Compared to 5-Fu's effect, BBPW-2 showed stronger inhibitory activity towards HeLa cells famous for extraordinary rapid proliferation, and exerted a highly significant effect ($P < 0.01$) above the of 1.0 mg/mL dose.

Crystal violet assay showed that the number of adherent MCF-7 cancer cells was decreased in a dose-dependent manner with BBPW-2 treatment for 8 days (Fig. 3C, D), which indicates that BBPW-2 has a durable anticancer effect on human breast cancer cells.

Emerging published papers has widely demonstrated that the anticancer activity of certain chemotherapeutic agents is related to apoptosis (Cao et al., 2010; Park et al., 2009) and cellcycle interruption (Shamtsyan et al., 2004). Considering the stronger inhibitory activity of BBPW-2 towards HeLa cells, further studies were conducted to explore the anticancer mechanism in the cell

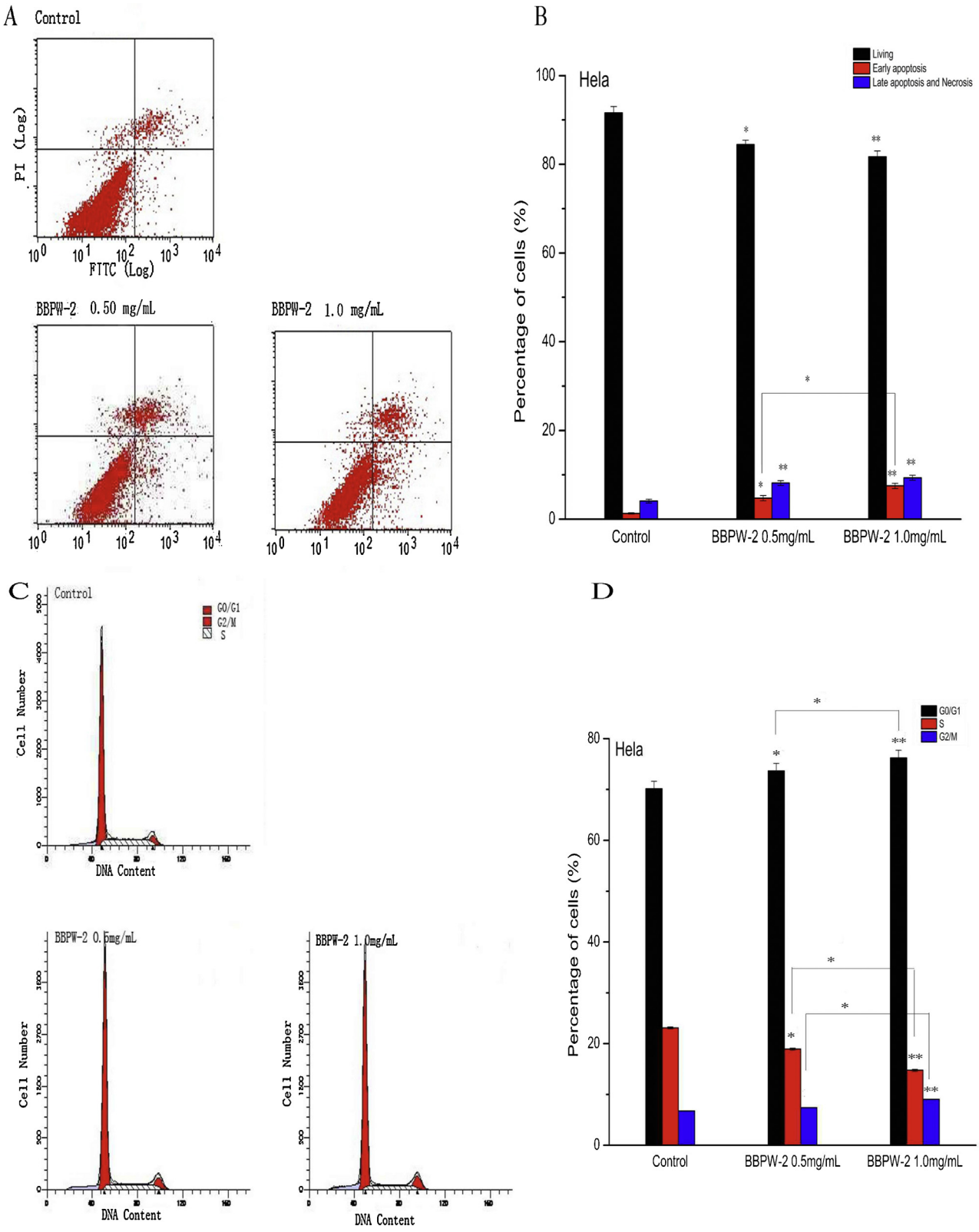

Fig. 4. Apoptosis analysis (A, B) and cellcycle analysis (C, D) of HeLa cells treated with BBPW-2 for 48 h.

line, including analysis of apoptosis and cellcycle. The apoptosis assessment of HeLa cells was carried out after a 48 h treatment with BBPW-2 at concentrations of 0.5 mg/mL and 1.0 mg/mL. A combination of Annexin V-FITC/PI kit and FACS analysis can distinguish viable cells, early apoptotic cells, late apoptotic and necrotic cells by staining of Annexin V^-/PI^- shown in the left-lower corner, Annexin V^+/PI^- in the right-lower corner, and Annexin V^+/PI^+ in the right-upper corner (Fig. 4A, B). As shown in Fig. 4, BBPW-2 enhanced the proportion of early apoptotic cells and late apoptotic cells, but decreased the living cells, when compared to control cells.

Table 3
Interglycosidic correlations from NOESY spectrum of BBPW-2.

Residue	Proton	Intra-correlation[a]
→2,6)-β-D-Man*p*(**c**)	H-1	3.98(**b**; H-4), 4.02(**b**; H-5)
→3)-α-D-Man*p*(**d**)	H-1	3.37(**f**; H-2)
→2,6)-α-D-glc*p*(**e**)	H-1	3.46(**a**; H-3)
β-D-Glc*p*(**f**)	H-1	3.98(**b**; H-4)

[a] Inter-residue NOEs are showed in bold font.

Table 4
Two and three-bond ^{1}H–^{13}C correlations for BBPW-2.

Residue	Proton	Proton correlation[a]
α-D-Man*p*(**a**)	H-1	76.8(**c**; C-5)
→2,6)-β-D-Man*p*(**c**)	H-1	71.3(**a**; C-4), 78.8(**d**; C-3)
→3)-α-D-Man*p*(**d**)	H-1	72.5(**f**; C-3)
→2,6)-β-D-glc*p*(**e**)	H-1	66.8(**a**; C-4),74.5(**b**; C-4)76.3(**f**; C-2)
β-D-Glc*p*(**f**)	H-1	74.5(**b**; C-4)

[a] Inter-residue correlations are shown in bold font.

These data indicated that BBPW-2 could induce apoptosis in HeLa cells.

The cellcycle of HeLa cells treated with BBPW-2 at the same concentration used for apoptosis analysis was differentiated in the respective phases (Fig. 4C, D). With respect to control cells, there was significant reduction in the frequency of cells in S phase and an increase in G0/G1 and G2/M phase after exposure to BBPW-2 for 48 h, suggesting that BBPW-2 reduced HeLa cells proliferation and this was associated with cellcycle arrest in the G0/G1 and G2/M phases.

4. Conclusions

A novel water soluble oligosaccharide BBPW-2 was purified from *B. batryticatus* by DEAE-Sepharose Fast Flow column and High-Resolution Sephacryl S-300 and S-200. This novel compound was identified by compositional, methylation and NMR analysis. The structural elucidation of BBPW-2 consisted of β-D-(1 → 2,6)-glucopyranose and β-D-(1 → 2,6)-mannosyl units as a backbone, α-D-(1 → 2)-galactopyranose and α-D-(1 → 3)-mannosyl units as branches, and α-D-Man*p* and β-D-Glc*p* as terminals.

In vitro antiproliferation studies of BBPW-2 against HeLa and HepG2 cell lines were conducted and it was found that BBPW-2 inhibited the growth of cancer cells at all concentrations, especially above 0.5 mg/mL. Crystal violet assays indicated that BBPW-2 caused durable growth inhibition of MCF-7 cancer cells. In our present study, BBPW-2 could induce cellcycle disruption in the G0/G1 and G2/M phases accompanied by an impressive increment of early apoptotic cells and late apoptotic and necrotic cells. These results suggest that BBPW-2 could be a potential chemotherapeutic drug candidate and its antitumor mechanism deserves further study.

Acknowledgments

This work was supported by the National Natural Science Foundation of China grant (31072090 and 31272375) and Zhejiang Sericultural Sci-Tech Innovation Team (2011R0028).

References

Anumula, K. R., & Taylor, P. B. (1992). A comprehensive procedure for preparation of partially methylated alditol acetates from glycoprotein carbohydrates. *Analytical Biochemistry*, *203*(1), 101–108.

Cao, W., Li, X. Q., Wang, X., Fan, H. T., Zhang, X. N., Hou, Y., Liu, S. B., & Mei, Q. B. (2010). A novel polysaccharide, isolated from *Angelica sinensis* (Oliv.) Diels induces the apoptosis of cervical cancer HeLa cells through an intrinsic apoptotic pathway. *Phytomedicine*, *17*(8–9), 598–605.

Chen, H. S., Tsai, Y. F., Lin, S., Lin, C. C., Khoo, K. H., Lin, C. H., & Wong, C. H. (2004). Studies on the immuno-modulating and anti-tumor activities of *Ganoderma lucidum* (Reishi) polysaccharides. *Bioorganic & Medicinal Chemistry*, *12*(21), 5595–5601.

Cui, J. J., Yuan, J. F., & Zhang, Z. Q. (2010). Anti-oxidation activity of the crude polysaccharides isolated from *Polygonum cillinerve* (Nakai) Ohwi in immunosuppressed mice. *Journal of Ethnopharmacology*, *132*(2), 512–517.

Dubois, M., Gilles, K. A., Hamilton, J. K., Rebers, P. A., & Smith, F. (1956). Colorimetric method for determination of sugars and related substances. *Analytical Chemistry*, *28*(3), 350–356.

Flick, D. A., & Gifford, G. E. (1984). Comparison of invitro-cell cyto-toxic assays for tumor necrosis factor. *Journal of Immunological Methods*, *68*(1–2), 167–175.

Gan, D., Ma, L. P., Jiang, C. X., Xu, R. J., & Zeng, X. X. (2011). Production, preliminary characterization and antitumor activity *in vitro* of polysaccharides from the mycelium of *Pholiota dinghuensis* Bi. *Carbohydrate Polymers*, *84*(3), 997–1003.

Jansson, P. E., Kenne, L., & Widmalm, G. (1989). Structure of the O-antigen polysaccharide from *Escherichia coli* 018AC – a revision using computer-assisted structural-analysis with the program casper. *Carbohydrate Research*, *193*, 322–325.

Kikuchi, H., Takahashi, N., & Oshima, Y. (2004). Novel aromatics bearing 4-O-methylglucose unit isolated from the oriental crude drug *Bombyx Batryticatus*. *Tetrahedron Letters*, *45*(2), 367–370.

Kim, H. J., Lee, W. H., Yoon, C. H., Jeong, J. C., Nam, K. S., Kim, H. M., Choo, Y. K., Lee, M. C., & Kim, C. H. (2001). *Bombycis corpus* extract prevents amyloid-beta-induced cytotoxicity and protects superoxide dismutase activity in cultured rat astrocytes. *Pharmacological Research*, *43*(1), 11–16.

Kim, Y. O., Park, H. W., Kim, J. H., Lee, J. Y., Moon, S. H., & Shin, C. S. (2006). Anti-cancer effect and structural characterization of endo-polysaccharide from cultivated mycelia of *Inonotus obliquus*. *Life Sciences*, *79*(1), 72–80.

Kodama, N., Murata, Y., & Nanba, H. (2004). Administration of a polysaccharide from *Grifola frondosa* stimulates immune function of normal mice. *Journal of Medicinal Food*, *7*(2), 141–145.

Kwon, H. C., Jung, I. Y., Cho, S. Y., Cho, O. R., Yang, M. C., Lee, S. O., Hur, J. Y., Kim, S. Y., Yang, J. B., & Lee, K. R. (2003). Phospholipids from *Bombycis corpus* and their neurotrophic effects. *Archives of Pharmacal Research*, *26*(6), 471–477.

Liao, C. H., Guo, S. J., & Lin, J. Y. (2011). Characterisation of the chemical composition and *in vitro* anti-inflammation assessment of a novel lotus (*Nelumbo nucifera* Gaertn) plumule polysaccharide. *Food Chemistry*, *125*(3), 930–935.

Mao, F., Xiao, B. X., Jiang, Z., Zhao, J. W., Huang, X., & Guo, J. M. (2011). Anticancer effect of *Lycium barbarum* polysaccharides on colon cancer cells involves G0/G1 phase arrest. *Medical Oncology*, *28*(1), 121–126.

Park, S. E., Yoo, H. S., Jin, C.-Y., Hong, S. H., Lee, Y.-W., Kim, B. W., Lee, S. H., Kim, W.-J., Cho, C. K., & Choi, Y. H. (2009). Induction of apoptosis and inhibition of telomerase activity in human lung carcinoma cells by the water extract of *Cordyceps militaris*. *Food and Chemical Toxicology*, *47*(7), 1667–1675.

Shamtsyan, M., Konusova, V., Maksimova, Y., Goloshchev, A., Panchenko, A., Simbirtsev, A., Petrishchev, N., & Denisova, N. (2004). Immunomodulating and anti-tumor action of extracts of several mushrooms. *Journal of Biotechnology*, *113*(1–3), 77–83.

Staaf, M., Urbina, F., Weintraub, A., & Widmalm, G. (1999). Structural elucidation of the O-antigenic polysaccharides from *Escherichia coli* O21 and the enteroaggregative *Escherichia coli* strain 105. *European Journal of Biochemistry*, *266*(1), 241–245.

Wu, J., Zhou, J. X., Lang, Y. G., Yao, L., Xu, H., Shi, H. B., & Xu, S. D. (2012). A polysaccharide from *Armillaria mellea* exhibits strong *in vitro* anticancer activity via apoptosis-involved mechanisms. *International Journal of Biological Macromolecules*, *51*(4), 663–667.

Xie, J. H., Liu, X., Shen, M. Y., Nie, S. P., Zhang, H., Li, C., Gong, D. M., & Xie, M. Y. (2013). Purification, physicochemical characterisation and anticancer activity of a polysaccharide from *Cyclocarya paliurus* leaves. *Food Chemistry*, *136*(3–4), 1453–1460.

Zhang, A. Q., Xu, M., Fu, L., & Sun, P. L. (2013). Structural elucidation of a novel mannogalactan isolated from the fruiting bodies of *Pleurotus geesteranus*. *Carbohydrate Polymers*, *92*(1), 236–240.